Available online at www.sciencedirect.com
SCIENCE DIRECT®
Atmospheric Environment 39 (2005) 3513–3520
ATMOSPHERIC ENVIRONMENT
www.elsevier.com/locate/atmosenv

Possible effect of boreal wildfire soot on Arctic sea ice and Alaska glaciers

Yongwon Kim[a,c,*], Hiroaki Hatsushika[b], Reginald R. Muskett[a], Koji Yamazaki[c]

[a]International Arctic Research Center, University of Alaska Fairbanks, Alaska, USA
[b]Environment Science Research Laboratory, Central Research Institute of Electric Power Industry, Japan
[c]Graduate School of Environmental Earth Science, Hokkaido University, Sapporo, Japan

Received 8 October 2004; accepted 8 February 2005

Abstract

The role of black carbon (BC) soot in the Arctic as an agent of climate warming through forcing/feedback of sea ice/glacier albedo is an uncertainty in need of addressing. In-situ measurements of BC-aerosols and gas byproducts from the FROSTFIRE experiment burn, 8–11 July 1999, are used with a coupled high-resolution wind field/empirical fall-out model to assess transport/dispersion and estimate deposition. Results suggest that BC-aerosols (soot) are quickly transported from central Alaska to the Arctic Ocean region of multi-year sea ice and to southern Alaska glaciers, where up to 20% can be deposited. The estimate of BC soot concentration from Alaska boreal wildfires favorably compares to in-situ sea ice observations made in 1998 and snow albedo observation on Gulkana Glacier in 2001. We hypothesize that northern boreal wildfires are a possible contributor in the reduction of first/multi-year sea ice/glacier extent by enhancing summer melting from albedo reduction. Should the occurrence and severity of northern boreal wildfires continue as in summer 2004, during which more than 670 km^2 burned and was the worst wildfire year on record, there will be implications for Northern hemisphere climate warming.

Keywords: Black carbon-aerosols; Climate warming; FROSTFIRE burning experiment; Trajectory model; Transport/deposition

1. Introduction

The late 20th century has witnessed the continuing effects of climate warming in the Northern Hemisphere (Levitus et al., 2001; Hansen et al., 2002). With increased air temperature over the North America boreal zone, the summer growing season and conditions favorable for wildfire have increased (Price and Rind, 1994; Grissom et al., 2000; Murphy et al., 2000; Jaffe et al., 2004). Stocks et al. (2000) predicted that the severity of boreal wildfire in Alaska and Canada would increase due to climate warming. A 50-year record of Alaska boreal fires shows an increase of fire occurrence and area burned (French et al., 2002). Records from Canada show much the same (Stocks et al., 2002). In the 1990s, the average area burned in Alaska was about 4×10^2 km^2 (Murphy et al., 2000). As of summer 2004, the total area burned in Alaska is more than 6×10^2 km^2 (Alaska Fire Service, http://fire.ak.blm.gov), clearly an extreme record. Jaffe et al. (2004) reported that the 2003 Russian forest burned area was 189×10^4 km^2, which was more than twice the annual average for Russian fires between 1996 and 2003, comparing to, or more likely larger than, 144×10^4 km^2 in Chinese fires in 1987 (Cahoon et al.,

*Corresponding author. Tel.: +1 907 474 2674; fax: +1 907 474 2679.
E-mail address: kimyw@iarc.uaf.edu (Y. Kim).

1352-2310/$ - see front matter © 2005 Elsevier Ltd. All rights reserved.
doi:10.1016/j.atmosenv.2005.02.050

1991) and $179 \times 10^4\,km^2$ in all boreal forest regions in 1998 (Kasischke and Bruhwiler, 2002).

Recent modeling indicates that soot is twice as effective as CO_2 in altering global surface air temperature and is capable of reducing sea ice and snow albedo (Hansen and Nazarenko, 2004). This affect could be contributing to trends toward early springs in the Northern Hemisphere, thinning Arctic sea ice and melting glaciers. Soot also plays a role in changes in the atmosphere by way altering the radiation balance through cloud formation. The implications suggest long-term climate and cryosphere consequences. However, is there a connection between northern boreal wildfires and Arctic sea ice/Alaska glacier extent reductions?

In this study, we report the results of modeling the FROSTFIRE experiment boreal forest control burn (Hinzman et al., 2003) regarding BC-aerosol/carbon-based gas transport/dispersion/deposition in the northern hemisphere. The results suggest that boreal wildfires are a major source of BC soot concentrations on Arctic multi-year sea ice and Alaska glaciers. We hypothesize that increased BC soot concentration is exacerbating summer melting of first/multi-year sea ice. Reduction in recruitment of first year into multi-year sea ice would lead to a reduction of sea ice extent. Increased BC soot concentrations on Alaska glaciers would increase summer melting and lead to reduction of glacier extent.

2. Aerosol–wind trajectory model

2.1. Wind field datasets

The principal datasets used in this study are the fine resolution European Center for Medium-Range Weather Forecast Tropical Ocean and Global Atmosphere (ECMWF/TOGA) objective analysis data (4 times per day, $0.5^\circ \times 0.5^\circ$ horizontal resolution at 15 pressure levels) during the period of 8–19 July 1999 (Fig. 1). The aerosol dispersion trajectories are modeled using horizontal wind and vertical p-velocity from the ECMWF datasets. The time step for the modeling calculations is 20 min. The three-dimensional wind fields are linearly interpolated at 20 min intervals from 6-h wind data. In the horizontal plane, winds are linearly interpolated to model particle locations, while the vertical winds are interpolated by a cubic spline interpolation procedure.

2.2. BC particle fall out velocity

We assume that a modeled particle falls at terminal velocity as a function of radius and density. Particle fallout velocity (V_f) is modeled as

$$V_f = -\beta \frac{m\alpha g}{k}\left(1 + 0.864\,\frac{\lambda}{r} + 0.29\,\frac{\lambda}{r}\exp\left(-1.25\,\frac{\lambda}{r}\right)\right),$$

which is a modified form of the fall velocity given by Kasten (1968). Model parameters are $k = 6\pi r\eta$, $\alpha = (\rho - \rho_o)/\rho$ and β, which accounts for non-spherical shape and is set to 0.5 for this study. Particle variables are density (ρ), radius (r) and mass (m). Atmosphere variables are density (ρ_o) and dynamic viscosity (η). The acceleration of gravity term is g. The particles are assumed to consist of BC soot. ρ_o is set to $1.65 \times 10^3\,kg\,m^{-3}$. The dynamic viscosity coefficient η is given as

$$\eta = \{0.046(T - T_0) + 17.1\} \times 10^{-6},$$

where T is air temperature and $T_0 = 273.15\,K$. λ is the mean free path given as

$$\lambda = \frac{kT}{4\sqrt{2}\pi r^2 P},$$

where k is the Boltzman constant of $1.381 \times 10^{-23}\,J\,K^{-1}$ and P is air pressure in kPa.

Originally, the model was developed from an empirical function (Fuchs, 1964) which is based on Stokes settling law modified by the Cunningham–Millikan correction for calculating the fall speed of a spherical particle in a gas of dynamic viscosity (η as above) given the particle radius and height above ground (Kasten, 1968). The coefficients in the expansion above, 0.86, 0.29 and 1.25, are dimensionless empirical constants determined by experiments and depend only on the mean free path λ. The acceleration of gravity has a small variation depending on the height above mean sea level and on geographic latitude. Using values of g, η and λ, Kasten (1968) numerically evaluated V_f for heights between 0 and 26 km in 1 km steps and for heights from 26 to 80 km in 2 km steps with particle radii of 0.003, 0.01, 0.03, 0.1, 0.3, and 10 μm and found the V_f justified for computing fall speed of aerosol particles in the atmosphere.

2.3. BC particle deposition

When the distance between a model particle and the ground becomes less than 10 hPa, we assume the particle settles by dry deposition. However, wet deposition (meteorological precipitation) obtained through VCR (Video Cassette Recorder) observations at Poker Flat Research Range of University of Alaska Fairbanks, and by meteorological observation at the weather station at Fairbanks Airport is incorporated by a simple procedure. In the ECMWF data used in this study, precipitation is itself not included. We first estimate the cloudiness from relative humidity as a linear function. Then the wet deposition rate is estimated from the cloudiness. When the cloudiness is 100%, the probability of wet deposition is 50% per hour and when the cloudiness is 50%, the probability is zero. Between 100% and 50% of cloudiness, the probability of wet

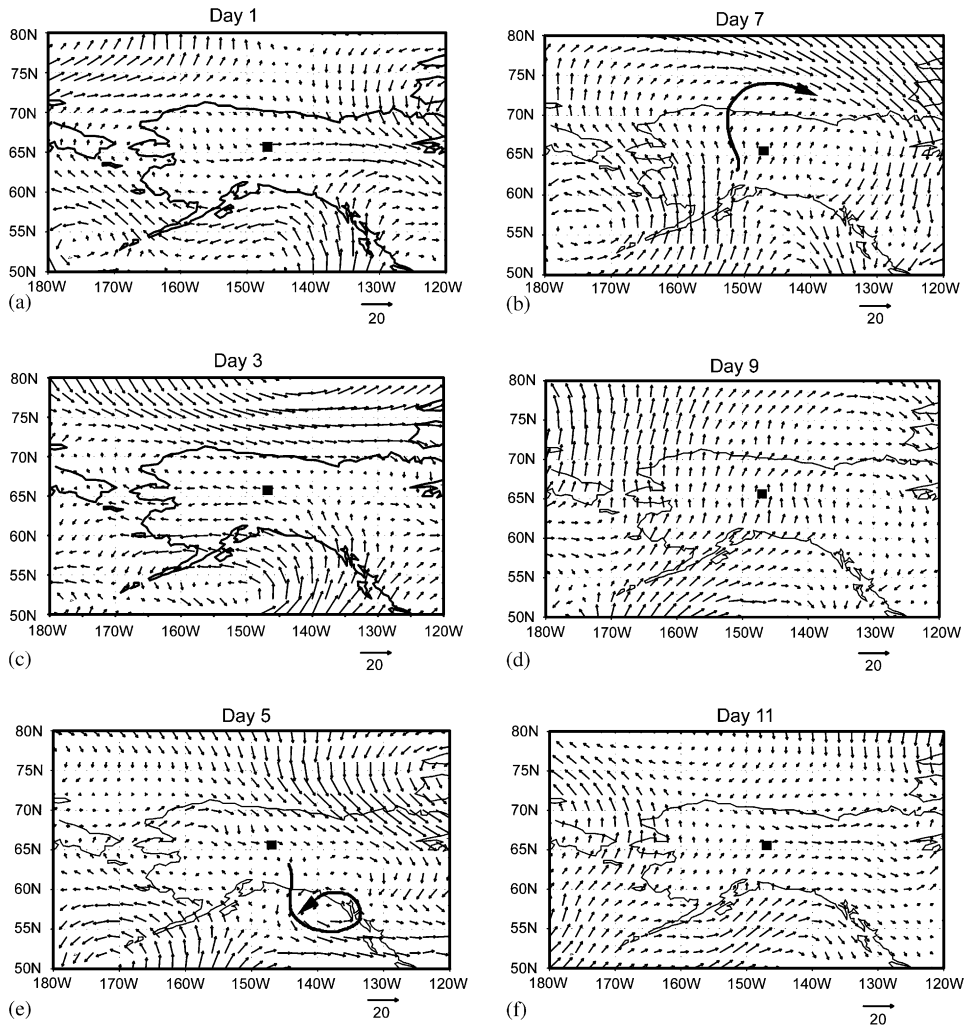

Fig. 1. Horizontal wind fields (ECMWF data) at 700 hPa, 00 UTC on day 1 (8 July) through day 12 (19 July). Arrow bar is 20 m s^{-1} wind velocity. Small black squares show the location of FROSTFIRE experiment site. (c) and (d) show a general flow path for particle transport being influenced by cyclonic and anti-cyclonic weather systems.

deposition is linearly interpolated. In the actual calculation, occurrence of wet deposition is determined using a random number with the humidity-dependent probability. Cloud scavenging/cycling is not directly modeled. Clark et al. (1996) showed that for the Central Arctic the annual cloud fraction ranges from about 55% to more than 80% with the peak spread over May to October. The peak of precipitation frequency occurs in September. The wet phase of precipitation peaks in July. This indicates our wet deposition rational is justified.

2.4. Trajectory model design

Using the uncertainty of the wind data and probability characteristics of the wet deposition scheme, we calculated a large number of trajectories of which particles are initially set over an area of $0.5^\circ \times 0.5^\circ$ in latitude and longitude, centered at the Little Poker Creek FROSTFIRE experiment site (65.2°N, 147.5°W). The lidar measurements, approximately 8 km from the burn site, detected smoke aerosols up to heights of about 2.5 km (Cahill and Collins, 2003). Model release time of gas/particle groups (gas with particles of 0.4, 1.0, 2, 5, 8, 10 and 20 μm radii sizes) was at specific hPa levels based on observed fire strength from about 23 UTC on 8 July to about 03 UTC on 11 July. Precipitation events were noted during VCR and ground observations at Poker Flat (Fukuda and Hayasaka, 2003). The wind directions as determined by in-situ observation were also recorded. The wind and precipitation observations agree with the

wind and relative humidity of the ECMWF objective analysis data.

Model particles were released for strong, medium and weak smoke cases (16,224, 11,494 and 6084; 295,412 total particles) at pressure levels of 700, 770 and 850 hPa, respectively, for eight times from 00 UTC 9 July to 00 UTC 11 July. Model runs were repeated for particle size varying from 0.4 to 20 μm in radius. An aerosol sampler measurement in the Caribou-Poker creek watershed revealed a size distribution that was significantly narrower than the typical log-normal distribution with a mean of about 0.4 μm.

3. Discussion

3.1. Prevailing wind field patterns

Fig. 1 shows the temporal variation of the horizontal wind field at 700 hPa over eastern Siberia–Alaska–Canada and the lower Arctic, from 50°N to 80°N and from 180°W to 120°W. Universal time is 00 UTC starting 9 July (a), day 1, through 19 July (f), day 11, 1999. In Fig. 1a (9 July), a westerly wind was dominant. In Fig. 1b (11 July), an easterly wind was dominant. During day 5 (Fig. 1c, 13 July) the wind was directed to the south. A general flow line is shown indicating particle transport being influenced by a cyclone passing west-to-east over southern Alaska and the Gulf of Alaska region. After that, a strong north-directed wind (Fig. 1d and e, 15–17, July) prevailed with the passage of an anticyclone. A general flow line shows transport north and over the Beaufort Sea and Arctic Ocean. Following the passage of the anticyclone, the wind direction changed back to westerly (Fig. 1f, 19 July).

Factors in the transport of the BC-aerosols to the Arctic and southern Alaska are northern and southern wind fields. We examined the mean and standard deviation of meridianal wind at 850 hPa with the ECMWF and NCEP reanalysis data (NOAA-CIRES CDC). Maps of the standard deviation were made for each month. July and August show the greatest probability of north and south directed winds $\geqslant 6\,\mathrm{m\,s^{-1}}$. Fig. 2 summarizes the monthly climatology (Va) and standard deviation (Vd) for zonal and meridional wind field at 700 hPa from 1979 to 2001. This is done by averaging winds of 4-time daily data. Eularian transport is to the north with positive Va + Vd. This implies that boreal fire will occur during dry conditions before the passage of an extratropical cyclone. On average, 1 day out of a week during the summer months will have strong north- or south-directed winds. This suggests that the transport of boreal wildfire BC-aerosols to the Arctic for deposition on multi-year sea ice is likely. Equally suggested is the transport and deposition of BC-aerosols to the glaciers

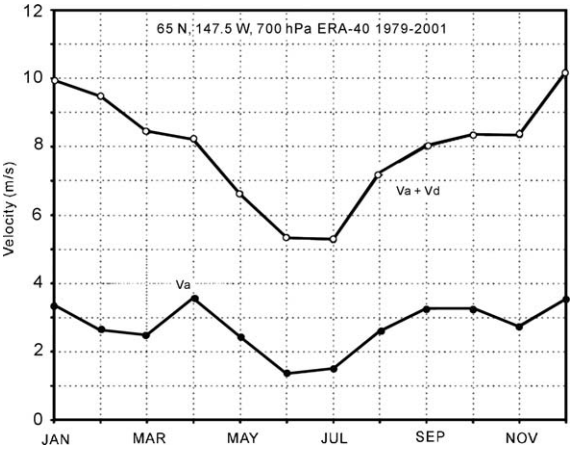

Fig. 2. Monthly mean climatology (Va) and standard deviation (Vd) for 4-time daily zonal and meridional wind field data from 1979 to 2001.

of southern Alaska and western Canada, which have undergone rapid melt in the later half of the 20th century and accelerated wasting from the 1990s to the present (Arendt et al., 2002; Muskett et al., 2003).

3.2. BC-aerosol 10 μm and gas distributions

Fig. 3 shows the area average density for gaseous materials and 10 μm particles in suspension and surface deposition through 19 July (day 11) at 00 UTC. Colors correspond to density in $\mathrm{g\,m^{-2}}$ based on the total BC-aerosol released by FROSTFIRE and mean area ($0.5^\circ \times 0.5^\circ$ grid cell) between 60°N and 80°N. By day 11 the gas and particle distributions covered much of the Arctic Ocean north of Alaska and Russia to as far west as north of the Barents Sea between Svalbard and Novaya Zemlya. Much of eastern Siberia, all of Alaska, and the Yukon Territory in Canada are covered. Portions of the gaseous distribution (Fig. 3a) reached as far south as 30°N off the west coast of North America to as far eastward as the eastern shore of Hudson Bay in Canada. The density of suspended (Fig. 3c) and deposited (Fig. 3d) 10 μm BC-aerosols are widely distributed in east Siberia, Alaska, and the Yukon, the Bering, Chukchi and Beaufort seas, and the Arctic Ocean. Moderate-to-high (green to orange) fall-out density occurs in a band 60°N to 85°N by 130°W to 180°W covering the large glaciers of southern Alaska to the Arctic Ocean where multi-year sea ice occurs.

In all cases of particle size from 0.4 to 10 μm, the deposition density is highest over central–southern Alaska (especially Gulkana Glacier in Alaska Range) and near the southern Yukon, where high-altitude snow cover is prominent. The BC deposited on snow can reduce the surface albedo and promote increased

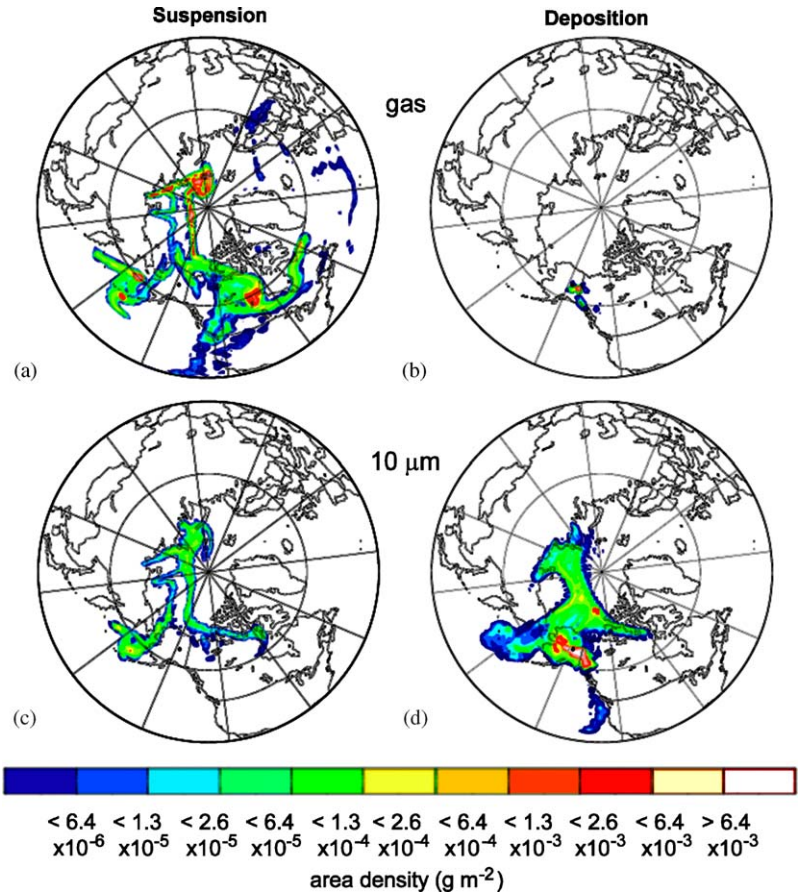

Fig. 3. Dispersion of carbon-based gas and BC aerosols on day 11 (19 July). Left/right plots show suspended and deposited gas/aerosols respectively. Scale is in density ($g\,m^{-2}$). Carbon-based gas is widely dispersed (a) but is restricted in deposition to Alaska (b). BC-aerosols size 10 μm are both widely dispersed (c) and deposited (d).

melting compared with clean snow (Warren and Wiscombe, 1980; Conway et al., 1996; Aoki et al., 2000; Takeuchi, 2002). This suggests that wildfires in Alaska may affect mountain snowpack and glacier ice wastage through albedo reduction during the summer ablation season (Hansen and Nazarenko, 2004).

3.3. BC-aerosol deposition in the northern hemisphere

Boreal wildfire BC-aerosols of moderate size can enter into the Arctic (first year and multi-year sea ice areas) and southern Alaska (largest connected glaciers and ice fields in continental North America) as shown in Fig. 3c and d for the 10 μm particles, and summarized in Fig. 4 for all particle sizes modeled. All particles with a radius size of 20 μm completely fall out in North America (south of 73°N) before 14 July, Fig. 4b. For particles less than 5 μm in size about 30% are deposited over much of North America by 19 July. Passage of the anticyclone over Alaska transports about 40% of the small particles to the Arctic Ocean and Alaska glaciers. About 28–45% of 8–0.4 μm and 7% of 10 μm particles can be transported to the Arctic Ocean (north) and Alaska glaciers (south) for deposition (Fig. 4b–d).

The albedo of snow is reduced by contamination of even a small amount of BC-aerosols, which subsequently increases melting (Conway et al., 1996; Hansen and Nazarenko, 2004). In the wavelength range of 0.28–2.8 μm, snow surfaces were treated with measured concentrations of submicron sized BC and volcanic ash. The initial snow surface (Blue Glacier, 47.8°N, 123.7°W, course gained, wet snow facies, 2050 m a.s.l., July through August 1991) albedo of 0.61 was reduced by 0.18 to about 0.43. Initial enhanced melting flushed a portion of the BC particles from the snowpack, leaving a residual concentration of about $5\times10^{-7}\,g\,C\,g^{-1}$ that persisted for several weeks. Compared to an untreated snow surface, the total albedo reduction was about 30%. This small amount of BC soot in the snowpack increased melting by 50% over the course of the experiment.

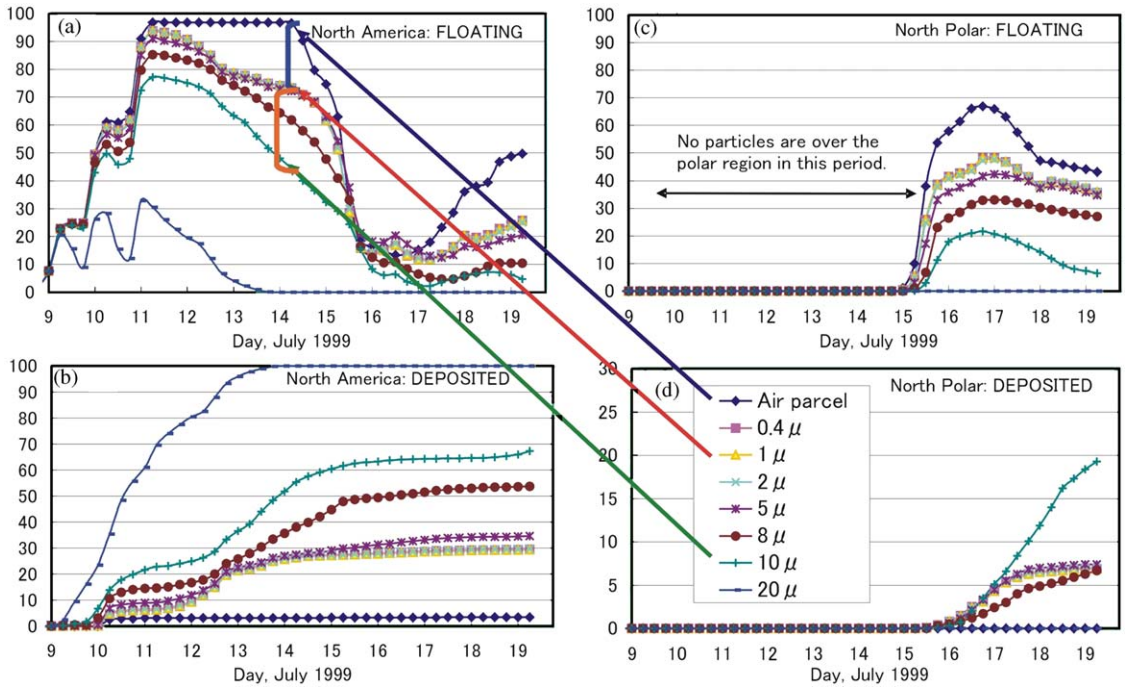

Fig. 4. Trajectory distributions, % of particles from release, 9 July through 19 July 1999. Panels (a, b) and (c, d) are divided geographically as those floating/deposited from 73°N to the equator and those floating/deposited from 73°N to the pole, respectively. The blue vertical bar, the difference in floating particles form air to 1 μm is mainly a function of precipitation, whereas the orange vertical bar difference is mainly a function of gravity settling (dry deposition).

Takeuchi (2002) reported on the surface albedo and characteristics of cryoconite (surface dust on glaciers) on the Gulkana Glacier in the Alaska Range. According to his results, the mean surface albedo of the glacier was 0.32 lower than 0.71 of clean snow. Moreover, microscopy results showed that cryoconite consisted of mineral particles, snow algae, and dark colored organic matter. The lowered surface albedo was by cryoconite and black carbon (BC) (e.g. soot) which could only have been transported to the glacier from long distance (see Fig. 3d).

The amount of total carbon released by FROSTFIRE was about 7×10^3 ton C with a burned area of about 4 km^2 (Alvarado and Sandberg, 2000). Hayasaka et al. (2000) also estimated a similar value. On the other hand, the average annual burned area in Alaska by wildfire in the 1990s was about 4×10^2 km^2 (Murphy et al., 2000). Therefore, the annual amount of total carbon released by forest fires in Alaska is about 7×10^5 ton C. The BC emission factor, i.e. the ratio of BC to total carbon in boreal forests is $1.2–1.5 \times 10^{-3}$ (Table 2 in Cooke and Wilson, 1996). Therefore, the annual release of BC is about $8.4–11 \times 10^2$ ton C. Our modeling shows that up to 7% of 0.4–8 μm and 20% of 10 μm BC-aerosols are deposited on the multi-year sea ice of the Arctic Ocean and the glaciers of southern Alaska. The mean area concentration of BC soot from Alaska sources on Arctic multi-year sea ice (4.0×10^{12} m^2 from Johannessen et al., 1999) is then about $0.2–0.6 \times 10^{-4}$ g m^{-2}. During the Surface Heat Budget of the Arctic Ocean (SHEBA) experiment, Arctic Ocean periphery observation (from Barrow, Alaska) of BC concentrations typically ranged from 4 to 5×10^{-4} g m^{-2} (Grenfell et al., 2002). Measurements on sea ice, April–March for background levels and 15 May 1998, north of Barrow, Alaska, ~76°N 165°W, averaged $4 \pm 3 \times 10^{-4}$ g m^{-2} within a 0.3 m thick snow layer. The estimated concentration of BC soot in this study is an order lower than those in Barrow observations suggesting sources from Canada, China, and Russia (see Fig. 1, Jaffe et al., 2004) in addition to Alaska.

A study of Arctic sites (6 excluding Greenland) conducted in 1983/4 showed an average of 30×10^{-4} g m^{-2} (Clarke and Noone, 1985) of BC soot. Monthly observations at Barrow, Alaska, conducted in 1989 (January to December) found BC soot in snow to vary from 2 to above 12×10^{-4} g m^{-2} with March showing the highest concentration in that year (Bodhaine, 1995). It has been suggested that the low BC soot concentration measured during SHEBA, compared to the 1983/1984 average, was attributable to the economic collapse of the Former Soviet Union and a general

decline in BC emissions from Eurasia in the 1990s, suggesting a strong anthropogenic source in addition to natural sources (Hansen and Nazarenko, 2004). However, Clark et al. (1996) showed that the SHEBA site in the Beaufort Sea was not characteristic of the Central Arctic which is cloudier, has higher frequency of precipitation and has lower temperatures.

4. Conclusions

This study describes modeling and analysis of in-situ BC-aerosol and soot observations of the FROSTFIRE experiment control burn in central Alaska. We used a high-resolution wind field, relative humidity and pressure level data sets with a physical model of BC-aerosol fall-out velocity. The modeling showed that BC-aerosol and soot particles of 0.4–10 μm radius can be transported to the Arctic region and the whole of Alaska in a very short time. There, deposition onto first and multi-year sea ice/northern high latitude glaciers by gravity fall-out and wet precipitation can occur. The modeled FROSTFIRE BC soot deposition on multi-year sea ice in the Arctic Ocean is up to $0.6 \times 10^{-4}\,\mathrm{g\,m^{-2}}$. This compares with an in-situ concentration of $4 \pm 3 \times 10^{-4}\,\mathrm{g\,m^{-2}}$ observed during the SHEBA experiment (Grenfell et al., 2002). The under-estimate of soot concentration suggests additional sources from boreal wildfires and human activities in the mid-to-high north latitudes. We hypothesize that the transport and deposition of boreal wildfire emitted BC-aerosols and soot to the Arctic and sub-Arctic regions can be an important natural contributor in the reduction of snow/ice albedo by causing increased melting of sea ice or glacier ice with the consequent reduction in sea ice extent and accelerated melting of glaciers.

BC-aerosol particles up to 10 μm in radius can have a long suspension time and thus potentially affect the albedo of the atmosphere and change the radiative balance (Campbell and Flannigan, 2000; Hansen and Nazarenko, 2004). They can also act as condensation nuclei to change normal precipitation patterns on a seasonal/annual basis (Sato et al., 2003). By changing the albedo and radiative balance of the Arctic cryosphere, boreal wildfires can directly affect global climate. Jaffe et al. (2004) pointed out that regional air quality and health were linked to global processes, including climate change, forest fires, and long-range transport of pollutants. Additional study on the Alaska wildfires is needed on the behavior of BC as well as trace gases (CO_2, CO, O_3, CH_4, and NMHCs) at a regional and global scale.

We plan additional investigations using the GEOS-CHEM global 3-D chemical transport model with the Naval Research Laboratory Aerosol Analysis and Prediction System combined with GOCART aerosol depth model and AERONET aerosol measurements (Martin et al., 2003; Jaffe et al., 2004). A final component of these investigations is to address the variability and influence of the North Pacific, Arctic and North Atlantic decadal oscillations on the trends of boreal wildfires. There is the suggestion that the large fires in coastal California chaparral in 2003 were linked to antecedent climate and meteorology conditions (Westerling et al., 2004). The correlation of large boreal wildfires with trends and shifts of climate regimes is yet to be established.

Acknowledgments

We thank Dr. L. Hinzman for encouragement and commentary, Dr. C.R. Duguay for valuable discussions and Mr. S. Maurits of the Arctic Region Supercomputing Center for assistance. We also thank two anonymous reviewers for beneficial comments. This research is a part of CREST projects provided by the Agency of Science and Technology (AST) and Japanese Science and Technology Corporation (PI: Dr. M. Fukuda, CREST Program).

References

Alaska Fire Service of Bureau of Land Management (BLM), 2004. http://fire.ak.blm.gov.

Alvarado, A., Sandberg, D.V., 2000. USDA Forest Service, dsandberg@fs.fed.us, personal communication.

Aoki, T., Fukabori, M., Hachikubo, A., Tachibana, Y., Nishio, F., 2000. Effects of snow physical parameters on spectral albedo and bidirectional reflectance of snow surface. Journal of Geophysical Research D105 (D8), 10,219–10,236.

Arendt, A.A., Echelmeyer, K.A., Harrison, W.D., Lingle, C.S., Valentine, V.B., 2002. Rapid wastage of Alaska glaciers and their contributions to rising sea level. Science 297, 382–389.

Bodhaine, B.A., 1995. Absorption-measurements at Barrow, Mauna-Loa and South-Pole. Journal of Geophysical Research 100 (D5), 8967–8975.

Cahill, C.F., Collins, R.L., 2003. University of Alaska Fairbanks, ffcfc@uaf.edu and rlc@gi.alaska.uaf.edu, personal communication.

Cahoon, D.R., Levine, J.S., Cofer III, W.R., Minnis, P., Miller, J.E., Tennile, G.M., Yip, W., Heck, P.W., Stocks, B.J., 1991. The great Chinese fire of 1987: a view from space. In: Levine, J.S. (Ed.), Global Biomass Burning: Atmospheric, Climate, and Biospheric Implications. MIT Press, Cambridge, pp. 61–66.

Campbell, I.D., Flannigan, M.D., 2000. Long-term perspectives on fire–climate–vegetation relationships in the North American boreal forest. In: Kasischke, E.S., Stock, B.J. (Eds.), Fire, Climate Change, and Carbon Cycling in the Boreal Forest. Ecological Studies, vol. 138. Springer, New York, pp. 151–172.

Clarke, A.D., Noone, K.J., 1985. Soot in the Arctic snowpack: a cause for perturbation in radiative transfer. Atmospheric Environment 19, 2045–2053.

Clark, M.P., Serreze, M.C., Berry, R.G., 1996. Characteristics of Arctic Ocean climate based on COADS data 1980–1993. Geophysical Research Letters 23 (15), 1953–1956.

Conway, H., Gades, A., Raymond, C.F., 1996. Albedo of dirty snow during conditions of melt. Water Resources Research 32 (6), 1713–1718.

Cooke, W.F., Wilson, J.N., 1996. A global black carbon aerosol model. Journal of Geophysical Research 101 (D14), 19,395–19,409.

French, N.H.F., Kasischke, E.S., Williams, D.G., 2002. Variability in the emission of carbon-based trace gases from wildfire in the Alaskan boreal forest. Journal of Geophysical Research 108 (D1), 8151.

Fuchs, N.A., 1964. The Mechanics of Aerosols. Pergamon Press, Oxford, pp. 27 and 31.

Fukuda, M., Hayasaka, H., 2003. Hokkaido University, mfukuda@pop.lowtem.hokudai.ac.jp, personal communication.

Grenfell, T.C., Light, B., Sturm, M., 2002. Spatial distribution and radiative effects of soot in the snow and sea ice during the SHEBA experiment. Journal of Geophysical Research 107 (C10).

Grissom, P., Alexander, M.E., Cella, B., Cole, F., Kurth, J.T., Malotte, N.P., Martell, D.L., Mawdsley, W., Roessler, J., Quillin, R., Ward, P.C., 2000. Effects of climate change on management and policy: mitigation options in the North American boreal forest. In: Kasischke, E.S., Stock, B.J. (Eds.), Fire, Climate Change, and Carbon Cycling in the Boreal Forest. Ecological Studies, vol. 138. Springer, New York, pp. 85–101.

Hansen, J., Nazarenko, L., 2004. Soot climate forcing via snow and ice albedos. Proceedings of the National Academy of Science 101 (2).

Hansen, J.E., Ruedy, R., Sato, M., Lo, K., 2002. Global warming continues. Science 295.

Hayasaka, H., Shinohara, M., Kudo, K., 2000. Forest fires in boreal forest—in case of Alaska taiga. Proceedings of the Joint Siberian Permafrost Studies between Japan and Russia, 2000, pp. 222–229.

Hinzman, L.D., Fukuda, M., Sandberg, D.V., Chapin III, F.S., Dash, D., 2003. FROSTFIRE: an experimental approach to predicting the climate feedbacks from the changing boreal fire regime. Journal of Geophysical Research 108 (D1).

Jaffe, D., Bertschi, I., Jaegle, L., Novelli, P., Reid, J.S., Tanimoto, H., Vingarzan, R., Westphal, D.L., 2004. Long-range transport of Siberian biomass burning emissions and impact on surface ozone in eastern North America. Geophysical Research Letters 31, L161606.

Johannessen, O.M., Shalina, E.V., Miles, M.W., 1999. Satellite evidence for an Arctic sea ice cover transformation. Science 386, 1937–1939.

Kasischke, E.S., Bruhwiler, L.P., 2002. Emission of carbon dioxide, carbon monoxide, and methane from boreal fires in 1998. Journal of Geophysical Research 108 (D1), 8146.

Kasten, F., 1968. Fall speed of aerosol particles. Journal of Applied Meteorology 7, 944–947.

Levitus, S., Antonov, J.I., Wang, J., Delworth, T.L., Dixon, K.W., Broccoli, A.J., 2001. Anthropogenic warming of Earth's climate system. Science 292, 267–277.

Martin, R.V., Jacob, D.J., Yantosca, R.M., Chin, M., Ginoux, P., 2003. Global and regional decreases in tropospheric oxidants from photochemical effects of aerosols. Journal of Geophysical Research 108 (D3), 4097.

Murphy, P.J., Mudd, J.P., Stocks, B.J., Kasischke, E.S., Barry, D., Alexander, M.E., French, N.H.F., 2000. Historical fire records in the North American boreal forest. In: Kasischke, E.S., Stock, B.J. (Eds.), Fire, Climate Change, and Carbon Cycling in the Boreal Forest. Ecological Studies, vol. 138. Springer, New York, pp. 274–288.

Muskett, R., Lingle, CS., Tangborn, W.V., Rabus, B.T., 2003. Multi-decadal elevation changes on Bagley Ice Valley and Malaspina Glacier, Alaska. Geophysical Research Letters 30 (16), 1857.

Price, C., Rind, D., 1994. The impact of a $2 \times CO_2$ climate on lightning-caused fires. Journal of Climate 7, 1484–1494.

Sato, M., Hansen, J., Koch, D., Lucis, A., Ruedy, R., Dubovik, O., Holben, B., Chin, M., Novakov, T., 2003. Global atmospheric black carbon inferred from AERONET. Proceedings of the National Academy of Science 100, 6319–6324.

Stocks, B.J., Fosberg, M.A., Wotton, M.B., Lynham, T.J., Ryan, K.C., 2000. Climate change and forest fire activity in North American boreal forests. In: Kasischke, E.S., Stock, B.J. (Eds.), Fire, Climate Change, and Carbon Cycling in the Boreal Forest. Ecological Studies, vol. 138. Springer, New York, pp. 368–376.

Stocks, B., Mason, J., Todd, J.B., Bosch, E.M., Wotton, B.M., Amiro, B.D., Flannigan, M.D., Hirsch, K.G., Logan, K.A., Martell, D.L., Skinner, W.R., 2002. Large forest fires in Canada, 1957–1997. Journal of Geophysical Research 107, 8149.

Takeuchi, N., 2002. Surface albedo and characteristics of cryoconite (biogenic surface dust) on an Alaska glacier. Gulkana Glacier in the Alaska Range. Bulletin of Glaciological Research 19, 63–70.

Warren, S.G., Wiscombe, W.J., 1980. A model for the spectral albedo of snow II, snow containing atmospheric aerosols. Journal of Atmospheric Science 37, 2734–2745.

Westerling, A.L., Can, A., Eustice, R., Lerner, S., McPhee, N., Pizarro, O., Roman, C., 2004. Climate, Santa Ana winds and autumn wildfires in southern California. EOS. Transactions of the American Geophysical Union 85 (31), 289 and 296.

Further reading

Ferguson, S., Collins, R.L., Ruthford, J., Fukuda, M., 2003. The vertical distribution of nighttime smoke following a wildland biomass fire in boreal Alaska. Journal of Geophysical Research 108 (D23), 4743.

Warren, S.G., Clarke, A.D., 1986. Soot from Arctic haze: radiative effects on the Arctic snowpack. Proceedings of the Snow Watch 85, Glaciological Data Report GD-18, pp. 73–77.